Rapid RF Flip Angle Imaging

D. Kim[1], S. Chung[1], D. K. Sodickson[1], and L. Axel[1]
[1]Radiology, New York University, New York, NY, United States

***Introduction*:** The transmit radiofrequency (RF) field (B_1) uniformity plays an important role in determining the image quality in MRI, particularly at high field strengths (≥ 3T). Accurate B_1 or flip angle maps are needed to compensate for B_1 variations through different correction methods such as signal normalization, RF shimming, or parallel RF excitation (i.e, transmit SENSE). Among the existing B_1 mapping methods, the double angle method (DAM) is most straightforward [1,2]. However, it is inefficient due to a need to set TR ≥ 5 T_1s. The image acquisition efficiency can be improved by performing saturation-recovery DAM, but is ultimately limited by a need to achieve sufficient magnetization recovery for adequate signal-to-noise ratio [3]. The purpose of this study is to develop a rapid in vivo B_1 mapping method based upon three single-shot image acquisitions.

***Methods*:** Our B_1 mapping method is based on a single-shot gradient echo (GRE) pulse sequence with two different k-space trajectories (i.e., phase reordering). According to the Bloch equation, the magnetization (M) of a non-steady state GRE sequence can be described as $M(k_y) = (E_1 \cos\theta)^{ky} + (1-E_1)(1-(E_1 \cos\theta)^{ky})/(1-E_1 \cos\theta)$, where $E_1 = e^{-TR/T1}$, θ = flip angle, equilibrium magnetization (M_0) =1, and k_y = phase-encoding line. Figure 1 shows plots of M as a function of k_y for the centric and reverse centric k-space trajectory image acquisitions at T_1 = 550ms and nominal flip angle =10°. The difference between the two M curves is the basis for B_1 sensitivity of our method. We define normalized signal as the ratio of reverse centric and centric k-space trajectory signals. As shown in Fig. 1B, the normalized signal is strongly high-pass filtered. To compensate for the high-pass filtering effects, we applied a Hanning window to the reverse centric k-space trajectory raw data prior to image normalization (Fig 1B). The resulting normalized signal has a relatively wide bandwidth in which its values are approximately the same as that of the origin of k-space. For convenience, we approximate the normalized image signal with a simplified theoretical function of M at the origin of k-space (Fig. 1C).

The three different images were acquired in the following order: centric k-space trajectory, followed by wait time of 5T_1s for magnetization recovery, reverse centric k-space trajectory, and saturation-recovery centric k-space trajectory. The pulse sequence with variable k-space trajectories was implemented on a 3T whole-body MR scanner (Tim Trio, Siemens). All experiments were conducted using a body-coil for RF transmit and a 12-channel phased array head coil for signal receive. Imaging parameters include: field of view = 300 x 300 mm, acquisition matrix = 128 x 128, spatial resolution = 2.3 x 2.3 mm, slice thickness = 8 mm, TE/TR = 1.3/2.6 ms, nominal flip angle = 10°, imaging time = 333 ms, and bandwidth = 750 Hz/pixel. A BIR-4 saturation pulse was used to perform uniform saturation of magnetization [4], and a saturation-recovery image was acquired with a time delay of 600 ms to estimate T_1. Total imaging time (including the wait time) = 333 ms + 5·T_1 + 333ms + 933 ms. DAM used similar imaging parameters except: nominal flip angle = 60/120°, TR = 5 T_1s, and bandwidth = 390 Hz/pixel. The total imaging time was 10·T_1·N_y, where N_y = total phase-encoding lines.

Phantom and in vivo experiments were performed to evaluate the relative accuracy of our method against DAM. We imaged a spherical oil phantom in a coronal plane and volunteers in a transverse plane of the brain. Human imaging was performed in accordance with protocols approved by the Human Investigation Committee at our institution. For image analysis, the ratio of DAM images was converted to flip angle as previously described [2]. For the new method, the Hanning-windowed reverse centric k-space image was divided by the centric k-space image, and the resulting normalized signal was converted to flip angle using the theoretical conversion function (Fig. 1C). The DAM and new flip angle maps were normalized by their respective nominal flip angles of 60° and 10°, respectively, because they were acquired with different flip angles. The relative accuracy of the normalized flip angle maps was evaluated by calculating the root-mean-square (RMS) error.

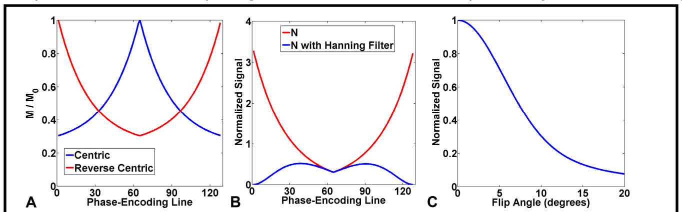

Fig. 1. (A) Plots of M as a function of k_y for the centric and reverse centric k-space trajectory images. (B) Normalized signal and hanning windowed signal for reduction of the k-space filtering effects. (C) Theoretical conversion function assuming signal = M at origin of k-space. T_1 = 550ms.

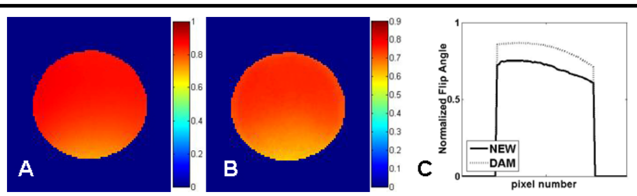

Fig. 2. Normalized flip angle maps for (A) DAM and (B) new method. (C) Vertical profiles of normalized flip angle along the middle of the phantom.

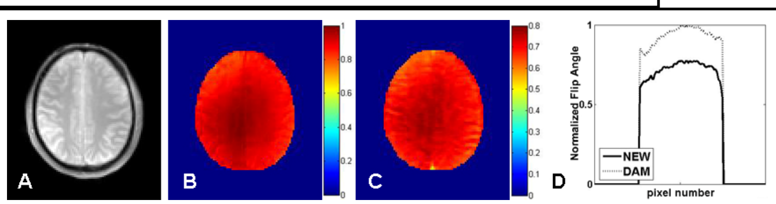

Fig. 3. (A) Brain image in a transverse plane. The corresponding normalized flip angle maps for (B) DAM and (C) new method. (D) Vertical profiles of normalized flip angle along the middle of the brain.

***Results*:** Figure 2 shows normalized flip angle maps of the phantom as well as their corresponding profiles. T_1 of the oil phantom was calculated as approximately 550 ms. The RMS error between the normalized flip angle maps of the phantom was 0.12. Figure 3 shows normalized flip angle maps of the brain as well as their corresponding profiles. The RMS error between the normalized flip angle maps of the brain was 0.20. While the RMS error values were relatively high, the two flip angle maps were qualitatively similar in terms of their shape. The new method consistently underestimated the flip angle compared with DAM, indicating that the results produced by the new method may contain a systematic error.

***Discussion*:** This study describes a new rapid in vivo B_1 mapping method that can be used for various B_1 compensation applications, including T_1 mapping and transmit SENSE. Our method is faster than DAM by a factor on the order of 2N_y (e.g., acceleration factor = 256 for N_y = 128). Compared with saturation-recovery DAM with TR = T_1, our method is faster by a factor on the order of 0.4N_y. However, our method consistently underestimated the flip angle by 12-20%. One possible cause for the underestimation of the flip angle is the signal variation due to the residual filtering effects (Fig. 1B). Another potential cause for the underestimation is true loss of RF transmit power during rapid imaging with short TR (i.e., unintended variable flip angle). Even with a small systematic offset, the possibility of rapidly imaging the shape of the flip angle distribution may be practically useful. Future work will include optimization of the sensitivity of the method to B_1, development of effective strategies to eliminate residual filtering effects, and characterization of the potential loss of RF transmit power during such rapid imaging.

References

1. Insko, EK and Bolinger, L. J Magn Reson A 1993; 103:82-85.
2. Strollberger, R et al. MRM 1996; 35:246-251.
3. Cunningham, CH et al. MRM 2006; 55:1326-1333.
4. Kim, D et al. MRM 2005; 54:1423-1429.